

Normalized Sombor indices as complexity measures of random graphs

R. Aguilar-Sánchez¹, J. A. Méndez-Bermúdez², José M. Rodríguez³, and José M. Sigarreta^{*4}

¹*Facultad de Ciencias Químicas, Benemérita Universidad Autónoma de Puebla, Puebla 72570, Mexico*

²*Instituto de Física, Benemérita Universidad Autónoma de Puebla, Apartado Postal J-48, Puebla 72570, Mexico*

³*Departamento de Matemáticas, Universidad Carlos III de Madrid, Avenida de la Universidad 30, 28911 Leganés, Madrid, Spain*

⁴*Facultad de Matemáticas, Universidad Autónoma de Guerrero, Carlos E. Adame No.54 Col. Garita, Acapulco Gro. 39650, Mexico*

ras747698@gmail.com, jmendezb@ifuap.buap.mx, jomaro@math.uc3m.es, jsmathguerrero@gmail.com

(Received xxx)

Abstract

We perform a detailed computational study of the recently introduced Sombor indices on random graphs. Specifically, we apply Sombor indices on three models of random graphs: Erdős-Rényi graphs, random geometric graphs, and bipartite random graphs. Within a statistical random matrix theory approach, we show that the average values of Sombor indices, normalized to the order of the graph, scale with the graph average degree. Moreover, we discuss the application of average Sombor indices as complexity measures of random graphs and, as a consequence, we show that selected normalized Sombor indices are highly correlated with the Shannon entropy of the eigenvectors of the graph adjacency matrix.

*Corresponding author

1 Introduction

Given a graph $G = (V(G), E(G))$, the Sombor index of G , introduced by I. Gutman in [1], is defined as

$$SO(G) = \sum_{uv \in E(G)} \sqrt{k_u^2 + k_v^2}, \quad (1)$$

where uv denotes the edge of the graph G connecting the vertices u and v and k_u is the degree of the vertex u . Also, the modified Sombor index of G was proposed in [2] as

$${}^m SO(G) = \sum_{uv \in E(G)} \frac{1}{\sqrt{k_u^2 + k_v^2}}. \quad (2)$$

In addition, two other Sombor indices have been introduced: the first Banhatti-Sombor index [3]

$$BSO(G) = \sum_{uv \in E(G)} \sqrt{\frac{1}{k_u^2} + \frac{1}{k_v^2}} \quad (3)$$

and the α -Sombor index [4]

$$SO_\alpha(G) = \sum_{uv \in E(G)} (k_u^\alpha + k_v^\alpha)^{1/\alpha}, \quad (4)$$

here $\alpha \in \mathbb{R}$. In fact, there is a general index that includes all the Sombor indices listed above: the first $(\alpha, \beta) - KA$ index of G which was introduced in [5] as

$$KA_{\alpha, \beta}^1(G) = \sum_{uv \in E(G)} (k_u^\alpha + k_v^\alpha)^\beta, \quad (5)$$

with $\alpha, \beta \in \mathbb{R}$. Note that $SO(G) = KA_{2, 1/2}^1(G)$, ${}^m SO(G) = KA_{2, -1/2}^1(G)$, $BSO(G) = KA_{-2, 1/2}^1(G)$, and $SO_\alpha(G) = KA_{\alpha, 1/\alpha}^1(G)$. Also, we note that $KA_{1, \beta}^1(G)$ equals the general sum-connectivity index [6] $\chi_\beta(G) = \sum_{uv \in E(G)} (k_u + k_v)^\beta$.

Reduced versions of $SO(G)$, ${}^m SO(G)$ and $KA_{\alpha, \beta}^1(G)$ were also introduced in [1, 2, 7]. However, when dealing with random graphs we use to approximate vertex degrees by average degrees and since average degrees may be less than one, reduced degree-based indices are not amenable for us. Thus we do not consider reduced Sombor indices here.

Even though Sombor indices were introduced very recently, there are already several works available in the literature where these indices are applied to chemical graphs of interest, see e.g. [4, 5, 7–18]. Also, bounds for Sombor indices as well as relations among them and with many other topological indices have been reported in [4, 10, 19–24]. From the application point of view, they have been shown to be useful to model entropy

and enthalpy of vaporization of alkanes [25]. In addition, the Sombor matrix has been proposed and studied in [26]. However, to the best of our knowledge, Sombor indices have not been applied to random graphs yet; thus in this work we undertake this task.

Here we consider three models of random graphs: Erdős-Rényi (ER) graphs, random geometric (RG) graphs, and bipartite random (BR) graphs. ER graphs [27–29] $G_{\text{ER}}(n, p)$ are formed by n vertices connected independently with probability $p \in [0, 1]$. While RG graphs [30, 31] $G_{\text{RG}}(n, r)$ consist of n vertices uniformly and independently distributed on the unit square, where two vertices are connected by an edge if their Euclidean distance is less or equal than the connection radius $r \in [0, \sqrt{2}]$. In addition we examine BR graphs $G_{\text{BR}}(n_1, n_2, p)$ composed by two disjoint sets, set 1 and set 2, with n_1 and n_2 vertices each such that there are no adjacent vertices within the same set, being $n = n_1 + n_2$ the total number of vertices in the bipartite graph. The vertices of the two sets are connected randomly with probability $p \in [0, 1]$.

We stress that the computational study of Sombor indices we perform here is justified by the random nature of the graph models we want to explore. Since a given parameter set $[(n, p), (n, r), \text{ or } (n_1, n_2, p)]$ represents an infinite-size ensemble of random [ER, RG, or BR] graphs, the computation of a Sombor index on a single graph is irrelevant. In contrast, the computation of a Sombor index on a large ensemble of random graphs, all characterized by the same parameter set, may provide useful *average* information about the full ensemble. This *statistical* approach, well known in random matrix theory studies, is not widespread in studies involving topological indices, mainly because topological indices are not commonly applied to random networks; for very recent exceptions see [32, 33].

Therefore, the purpose of this work is threefold. First, we push forward the statistical (computational) analysis of topological indices as a generic tool for studying average properties of random graphs; second, we perform for the first time (to our knowledge), a scaling study of Sombor indices on random graphs; and third, we discuss the application of selected Sombor indices as complexity measures of random graphs.

2 Computational properties of Sombor indices on random graphs

2.1 Sombor indices on Erdős-Rényi graphs

In what follows we present the average values of the indices defined in Eqs. (1-5). All averages are computed over ensembles of $10^7/n$ ER graphs characterized by the parameter pair (n, p) .

On the one hand, in Figs. 1(a), 1(b), and 1(c) we present, respectively, the average Sombor index $\langle SO(G_{\text{ER}}) \rangle$, the average modified Sombor index $\langle {}^m SO(G_{\text{ER}}) \rangle$, and the average first Bhatti-Sombor index $\langle BSO(G_{\text{ER}}) \rangle$ as a function of the probability p of ER graphs of sizes $n = \{125, 250, 500, 1000\}$. On the other hand, in Fig. 2 we plot the average α -Sombor index $\langle SO_\alpha(G_{\text{ER}}) \rangle$, see Fig. 2(a), and the average first $(\alpha, \beta) - KA$ index $\langle KA_{\alpha, \beta}^1(G_{\text{ER}}) \rangle$, see Figs. 2(c,d), as a function p of ER graphs of size $n = 1000$. In Fig. 2 we show curves for $\alpha \in [-2, 2]$ and, in the case of $\langle KA_{\alpha, \beta}^1(G_{\text{ER}}) \rangle$, we choose to report $\beta = 1/2$ and $\beta = 2$ as representative cases.

From this figures we observe that:

- (i) The curves of $\langle SO(G_{\text{ER}}) \rangle$ and $\langle SO_\alpha(G_{\text{ER}}) \rangle$ are monotonically increasing functions of p . See Figs. 1(a) and 2(a).
- (ii) The curves of $\langle {}^m SO(G_{\text{ER}}) \rangle$ and $\langle BSO(G_{\text{ER}}) \rangle$ grow for small p and saturate above a given value of p . See Figs. 1(b) and 1(c).
- (iii) The curves of $\langle KA_{\alpha, \beta}^1(G_{\text{ER}}) \rangle$ show three different behaviors as a function of p depending on the values of α and β : For $\alpha < \alpha_0$, they grow for small p , approach a maximum value and then decrease when p is further increased. For $\alpha > \alpha_0$, they are monotonically increasing functions of p . For $\alpha = \alpha_0$ the curves saturate above a given value of p . For $\beta = 1/2$ and $\beta = 2$, the cases reported in Figs. 2(c,d), we found $\alpha_0 = -2$ and $\alpha_0 = -1/2$, respectively.
- (iv) When $np \gg 1$, we can approximate $k_u \approx k_v \approx \langle k \rangle$ in Eqs. (1-5), with

$$\langle k \rangle = (n - 1)p. \quad (6)$$

Therefore, for $np \gg 1$, the average values of the Sombor indices are well approximated by:

$$\langle SO(G_{\text{ER}}) \rangle \approx \frac{n}{\sqrt{2}} [(n - 1)p]^2, \quad (7)$$

$$\langle {}^m SO(G_{\text{ER}}) \rangle \approx \frac{n}{2\sqrt{2}}, \quad (8)$$

$$\langle BSO(G_{\text{ER}}) \rangle \approx \frac{n}{\sqrt{2}}, \quad (9)$$

$$\langle SO_\alpha(G_{\text{ER}}) \rangle \approx \frac{n}{2^{1-1/\alpha}} [(n-1)p]^2, \quad (10)$$

$$\langle KA_{\alpha,\beta}^1(G_{\text{ER}}) \rangle \approx \frac{n}{2^{1-\beta}} [(n-1)p]^{1+\alpha\beta}. \quad (11)$$

In Figs. 1(a)-1(c), we show that Eqs. (7-9) (dashed lines) indeed describe well the data (thick full curves) for large enough p . We also verified that Eqs. (10,11) describe well the data for $np \gg 1$ reported in Figs. 2(a-c), however we did not include them to avoid figure saturation.

We note that in Figs. 1(a-c) we present average Sombor indices as a function of the probability p of ER graphs of four different sizes n . It is quite clear from these figures that the curves, characterized by the different network sizes, are very similar but displaced on both axes. A similar observation can be made for $\langle SO_\alpha(G_{\text{ER}}) \rangle$ and $\langle KA_{\alpha,\beta}(G_{\text{ER}}) \rangle$ (not shown in Figs. 2(a-c) to avoid figure saturation). This behavior suggests that the average Sombor indices can be scaled. Then, in what follows we look for the parameters that scale the average Sombor indices.

From Eqs. (7-11) we observe that $\langle X(G_{\text{ER}}) \rangle \propto nf[(n-1)p]$ or

$$\langle X(G_{\text{ER}}) \rangle \propto nf(\langle k \rangle), \quad (12)$$

where X represents all the Sombor indices studied here. Therefore, in Figs. 1(d-f) and 2(d-f) we plot average Sombor indices, normalized to n , as a function of $\langle k \rangle$ showing that all indices are now properly scaled; i.e. the curves painted in different colors for different graph sizes fall on top of each other. Moreover, we can rewrite Eqs. (7-11) as

$$\frac{\langle SO(G_{\text{ER}}) \rangle}{n} \approx \frac{1}{\sqrt{2}} \langle k \rangle^2, \quad (13)$$

$$\frac{\langle {}^m SO(G_{\text{ER}}) \rangle}{n} \approx \frac{1}{2\sqrt{2}}, \quad (14)$$

$$\frac{\langle BSO(G_{\text{ER}}) \rangle}{n} \approx \frac{1}{\sqrt{2}}, \quad (15)$$

$$\frac{\langle SO_\alpha(G_{\text{ER}}) \rangle}{n} \approx \frac{1}{2^{1-1/\alpha}} \langle k \rangle^2, \quad (16)$$

$$\frac{\langle KA_{\alpha,\beta}^1(G_{\text{ER}}) \rangle}{n} \approx \frac{1}{2^{1-\beta}} \langle k \rangle^{1+\alpha\beta}. \quad (17)$$

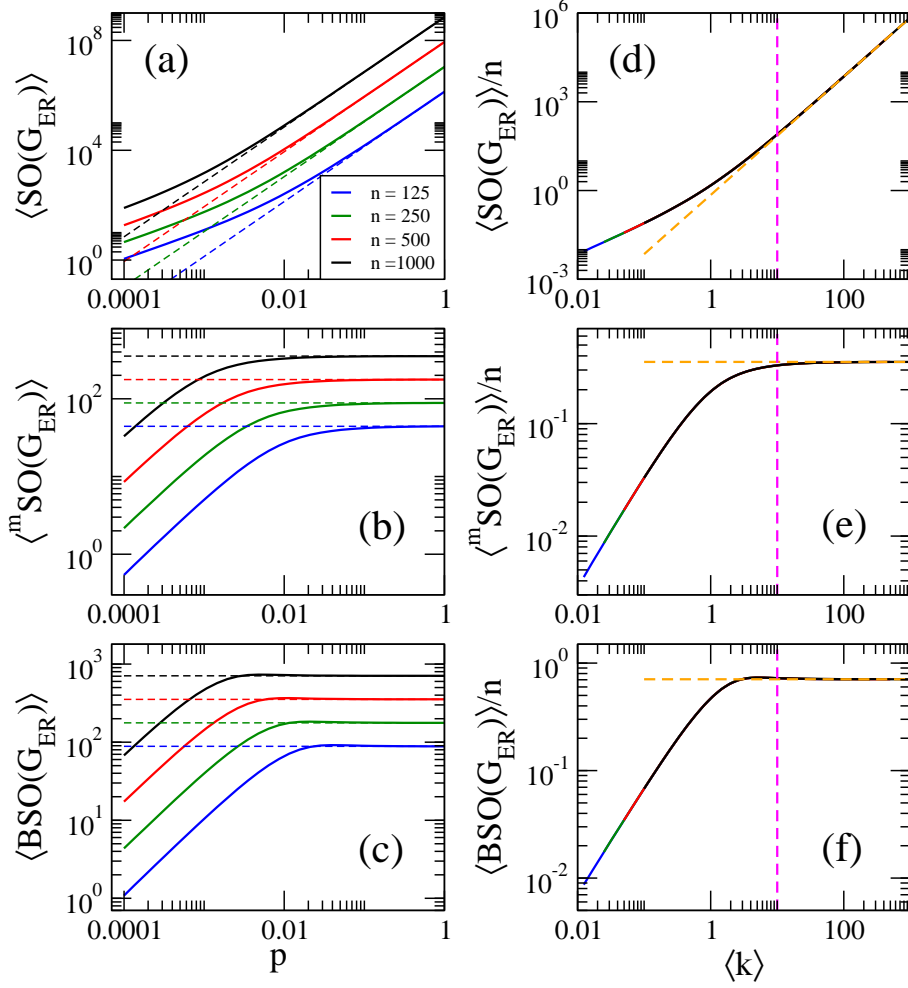


Figure 1. (a) Average Sombor index $\langle SO(G_{ER}) \rangle$, (b) average modified Sombor index $\langle {}^m SO(G_{ER}) \rangle$, and (c) average first Banhatti-Sombor index $\langle BSO(G_{ER}) \rangle$ as a function of the probability p of Erdős-Rényi graphs of size n . (d) $\langle SO(G_{ER}) \rangle / n$, (e) $\langle {}^m SO(G_{ER}) \rangle / n$, and (f) $\langle BSO(G_{ER}) \rangle / n$ as a function of $\langle k \rangle$. Dashed lines in panels (a), (b) and (c) correspond to Eqs. (7), (8) and (9), respectively. While dashed lines in panels (d), (e) and (f) are Eqs. (13), (14) and (15), respectively. The vertical magenta dashed line in (b-f) marks $\langle k \rangle = 10$.

In Figs. 1(d)-1(f), we show that Eqs. (13-15) (orange-dashed lines) indeed describe well the data (thick full curves) for $\langle k \rangle \geq 10$. We also verified that Eqs. (16-17) describe well the data for $\langle k \rangle \geq 10$ reported in Figs. 2(d)-2(f) (not shown here to avoid figure saturation).

It is relevant to stress that even when Eq. (12) was deduced from Eqs. (7-11), expected to be valid in the dense limit (i.e. for $\langle k \rangle \gg 1$), it is indeed valid for any $\langle k \rangle$ as clearly seen in Figs. 1(d)-1(f) and Figs. 2(d)-2(f).

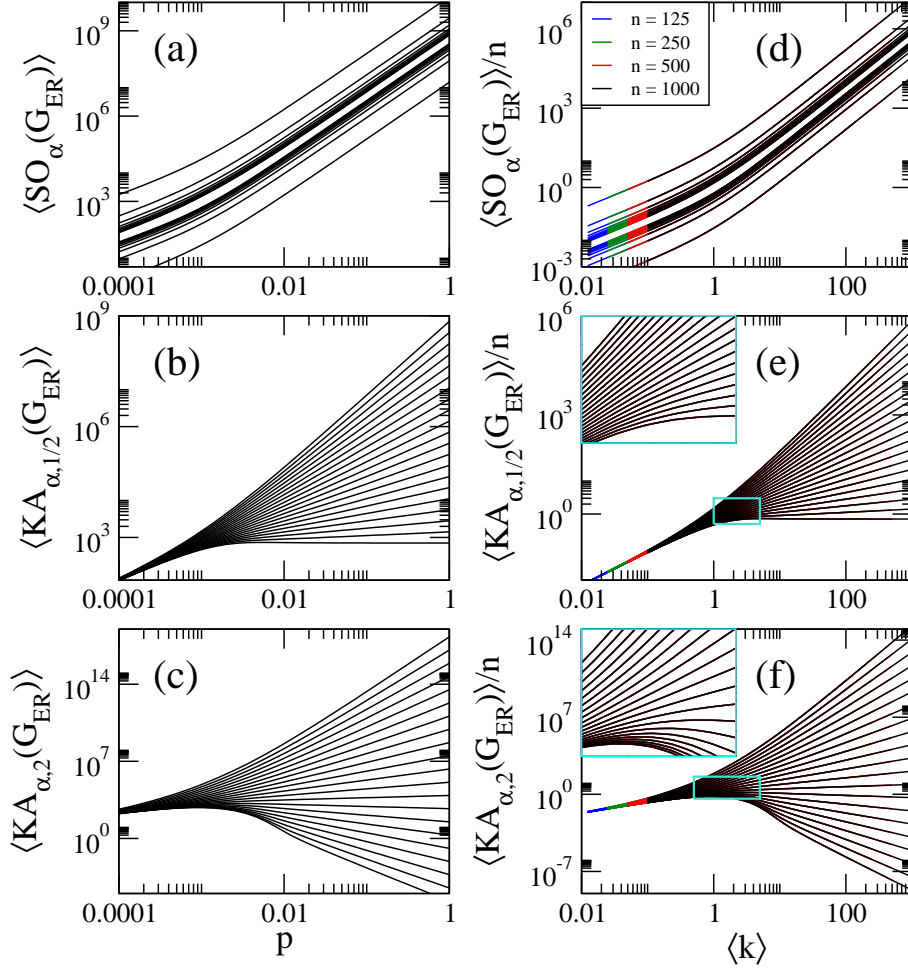


Figure 2. (a) Average α -Sombor index $\langle SO_\alpha(G_{ER}) \rangle$, (b) average first $(\alpha, \beta) - KA$ index $\langle KA_{\alpha, \beta}(G_{ER}) \rangle$, with $\beta = 1/2$, and (c) average first $(\alpha, \beta) - KA$ index $\langle KA_{\alpha, \beta}(G_{ER}) \rangle$, with $\beta = 2$, as a function of the probability p of Erdős-Rényi graphs of size $n = 1000$. In all panels we show curves for $\alpha \in [-2, 2]$ in steps of 0.2 (from bottom to top). (d) $\langle SO_\alpha(G_{ER}) \rangle / n$, (e) $\langle KA_{\alpha, 1/2}(G_{ER}) \rangle / n$, and (f) $\langle KA_{\alpha, 2}(G_{ER}) \rangle / n$ as a function of $\langle k \rangle$ for ER graphs of four different sizes n . The insets in (e,f) are enlargements of the cyan rectangles.

2.2 Sombor indices on random geometric graphs

As in the previous Subsection, here we present the average values of the Sombor indices listed in Eqs. (1-5). Again, all averages are computed over ensembles of $10^7/n$ random graphs, each ensemble characterized by a fixed parameter pair (n, r) .

Then, in Figs. 3(a), 3(b), and 3(c) we present, respectively, the average Sombor index $\langle SO(G_{RG}) \rangle$, the average modified Sombor index $\langle {}^m SO(G_{RG}) \rangle$, and the average first Banhatti-Sombor index $\langle BSO(G_{RG}) \rangle$ as a function of the connection radius r of RG graphs of sizes $n = \{125, 250, 500, 1000\}$. Also, in Fig. 4 we plot the average α -Sombor index $\langle SO_\alpha(G_{RG}) \rangle$, see Fig. 4(a), and the average first $(\alpha, \beta) - KA$ index $\langle KA_{\alpha, \beta}^1(G_{RG}) \rangle$, see

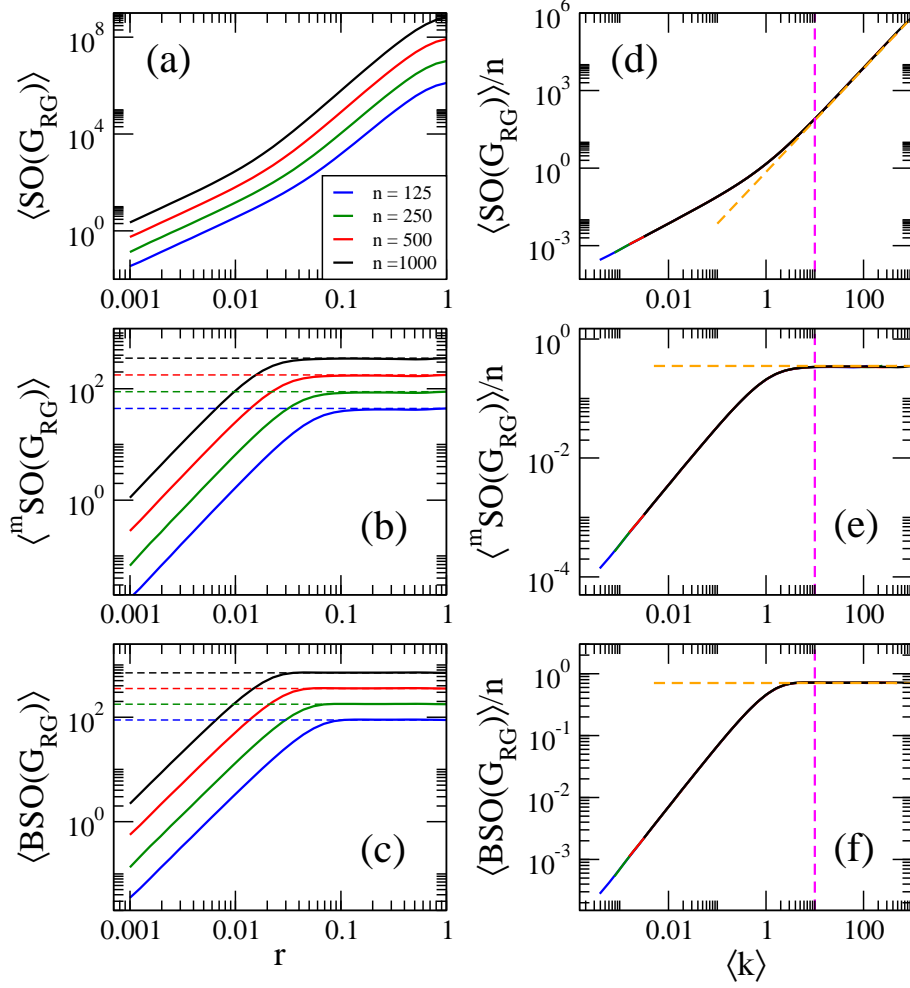


Figure 3. (a) Average Sombor index $\langle SO(G_{RG}) \rangle$, (b) average modified Sombor index $\langle {}^m SO(G_{RG}) \rangle$, and (c) average first Bhatti-Sombor index $\langle BSO(G_{RG}) \rangle$ as a function of the connection radius r of random geometric graphs of size n . (d) $\langle SO(G_{RG}) \rangle / n$, (e) $\langle {}^m SO(G_{RG}) \rangle / n$, and (f) $\langle BSO(G_{RG}) \rangle / n$ as a function of $\langle k \rangle$. Dashed lines in panels (a), (b) and (c) correspond to Eqs. (20), (21) and (22), respectively. While dashed lines in panels (d), (e) and (f) are Eqs. (13), (14) and (15), respectively. The vertical magenta dashed line in (b-f) marks $\langle k \rangle = 10$.

Figs. 4(c,d), as a function r of RG graphs of size $n = 1000$.

For comparison purposes, Figs. 3 and 4 are similar to Figs. 1 and 2. In fact, all the observations (i-iv) made in the previous Subsection for ER graphs are also valid for RG graphs by replacing $G_{ER} \rightarrow G_{RG}$ and $p \rightarrow g(r)$, with [34]

$$g(r) = \begin{cases} r^2 \left[\pi - \frac{8}{3}r + \frac{1}{2}r^2 \right] & 0 \leq r \leq 1, \\ \frac{1}{3} - 2r^2 \left[1 - \arcsin(1/r) + \arccos(1/r) \right] + \frac{4}{3}(2r^2 + 1)\sqrt{r^2 - 1} - \frac{1}{2}r^4 & 1 \leq r \leq \sqrt{2}. \end{cases} \quad (18)$$

However, given the fact that this is the first study (to our knowledge) of average Sombor indices on RG graphs, we want to stress that when $nr \gg 1$, we can approximate $k_u \approx$

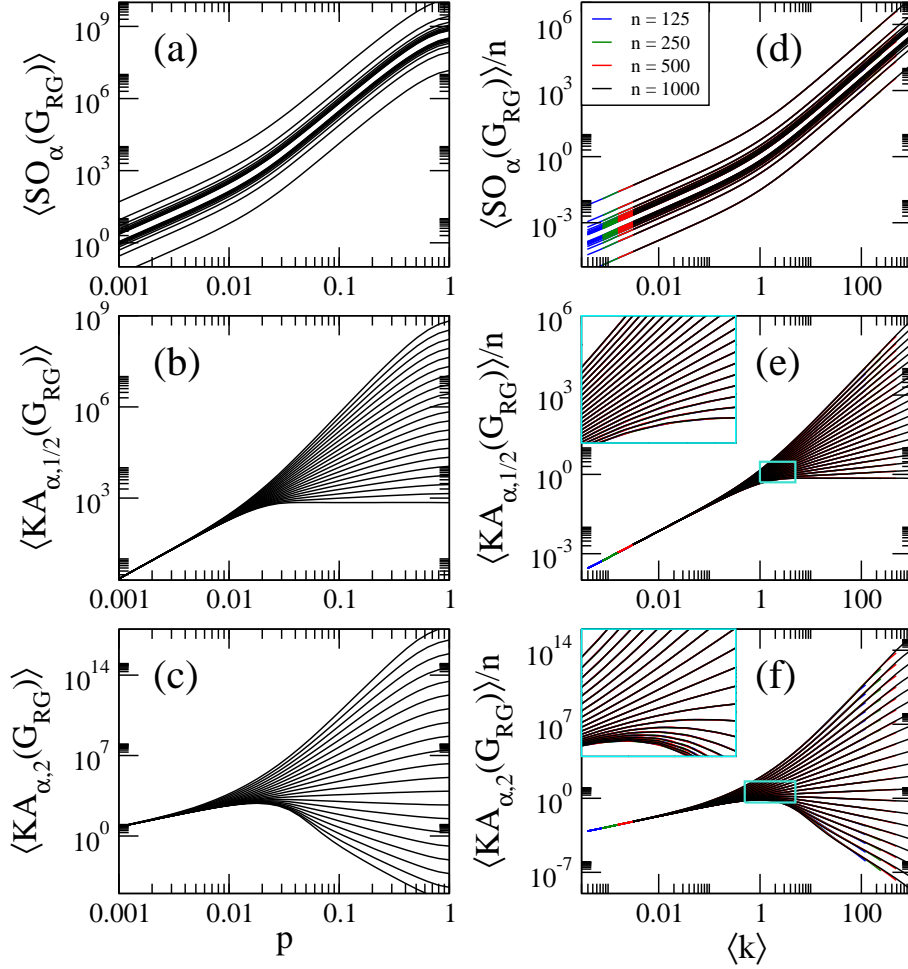


Figure 4. (a) Average α -Sombor index $\langle SO_\alpha(G_{\text{RG}}) \rangle$, (b) average first (α, β) - KA index $\langle KA_{\alpha, \beta}(G_{\text{RG}}) \rangle$, with $\beta = 1/2$, and (c) average first (α, β) - KA index $\langle KA_{\alpha, \beta}(G_{\text{RG}}) \rangle$, with $\beta = 2$, as a function of the connection radius r of random geometric graphs of size $n = 1000$. In all panels we show curves for $\alpha \in [-2, 2]$ in steps of 0.2 (from bottom to top). (d) $\langle SO_\alpha(G_{\text{RG}}) \rangle / n$, (e) $\langle KA_{\alpha, 1/2}(G_{\text{RG}}) \rangle / n$, and (f) $\langle KA_{\alpha, 2}(G_{\text{RG}}) \rangle / n$ as a function of $\langle k \rangle$ for RG graphs of four different sizes n . The insets in (e,f) are enlargements of the cyan rectangles.

$k_v \approx \langle k \rangle$ in Eqs. (1-5), with

$$\langle k \rangle = (n - 1)g(r). \quad (19)$$

Therefore, in the dense limit, the average values of the Sombor indices on RG graphs are well approximated by:

$$\langle SO(G_{\text{RG}}) \rangle \approx \frac{n}{\sqrt{2}} [(n - 1)g(r)]^2, \quad (20)$$

$$\langle {}^m SO(G_{\text{RG}}) \rangle \approx \frac{n}{2\sqrt{2}}, \quad (21)$$

$$\langle BSO(G_{\text{RG}}) \rangle \approx \frac{n}{\sqrt{2}}, \quad (22)$$

$$\langle SO_\alpha(G_{\text{RG}}) \rangle \approx \frac{n}{2^{1-1/\alpha}} [(n - 1)g(r)]^2, \quad (23)$$

$$\langle KA_{\alpha,\beta}^1(G_{\text{RG}}) \rangle \approx \frac{n}{2^{1-\beta}} [(n-1)g(r)]^{1+\alpha\beta}. \quad (24)$$

In Figs. 3(a)-3(c), we show that Eqs. (20-22) (dashed lines) indeed describe well the data (thick full curves) for large enough r . We also verified that Eqs. (23,24) describe well the data reported in Figs. 4(a-c), for large enough r , however we did not include them to avoid figure saturation.

It is quite remarkable to note that by substituting the average degree of Eq. (19) into Eqs. (20-22) we get exactly the same expressions listed in Eqs. (13-17). Therefore, in Figs. 3(d-f) and 4(d-f) we plot average Sombor indices, on RG graphs, normalized to n , as a function of $\langle k \rangle$ showing that all curves are properly scaled. Also, in Figs. 3(d)-3(f), we show that Eqs. (13-15) (orange-dashed lines) indeed describe well the data (thick full curves) for $\langle k \rangle \geq 10$. We also verified (not shown here) that Eqs. (16-17) describe well the data for $\langle k \rangle \geq 10$ reported in Figs. 2(d)-2(f).

2.3 Sombor indices on bipartite random graphs

Now we compute average Sombor indices on ensembles of $10^7/n$ BR graphs. In contrast to ER and RG graphs now the BR graph ensembles are characterized by three parameters: n_1 , n_2 , and p . Thus we consider two cases: $n_1 = n_2$ and $n_1 < n_2$. We note that bounds for the Sombor index on bipartite graphs have been reported in [21].

In Figs. 5(a), 5(b), and 5(c) we present, respectively, the average Sombor index $\langle SO(G_{\text{BR}}) \rangle$, the average modified Sombor index $\langle {}^m SO(G_{\text{BR}}) \rangle$, and the average first Banhatti-Sombor index $\langle BSO(G_{\text{BR}}) \rangle$ as a function of the probability p of BR graphs characterized by $n_1 = n_2$ with $n_2 = \{125, 250, 500, 1000\}$ (blue lines) and BR graphs characterized by $n_1 < n_2$ with $n_1 = 125$ and $n_2 = \{125, 250, 500, 1000\}$ (red lines). Also, in Fig. 6 we plot the average α -Sombor index $\langle SO_\alpha(G_{\text{BR}}) \rangle$, see Fig. 6(a), and the average first (α, β) -KA index $\langle KA_{\alpha,\beta}^1(G_{\text{BR}}) \rangle$, see Figs. 6(c,d), as a function p of BR graphs of size $n_1 = n_2 = 1000$.

It is interesting to notice that all the observations (**i-iv**) made in Subsection 2.2 for ER graphs are also valid for BR graphs by just replacing $G_{\text{ER}} \rightarrow G_{\text{BR}}$. Moreover, we can also write approximate expressions for the average Sombor indices on BR graphs in the dense limit. However, since edges in a bipartite graph join vertices of different sets, and we are labeling here the sets as set 1 and set 2, we replace d_u by d_1 and d_v by d_2 in the expression for the Sombor indices. Thus, when $n_1 p \gg 1$ and $n_2 p \gg 1$, we can

approximate $k_u = k_1 \approx \langle k_1 \rangle$ and $k_v = k_2 \approx \langle k_2 \rangle$ in Eqs. (1-5), with

$$\langle k_{1,2} \rangle = n_{2,1}p. \quad (25)$$

Therefore, in the dense limit, the average values of the Sombor indices on BR graphs are well approximated by:

$$\langle SO(G_{\text{BR}}) \rangle \approx \sqrt{n_1^2 + n_2^2} (n_1 n_2)^2 p^4, \quad (26)$$

$$\langle {}^m SO(G_{\text{BR}}) \rangle \approx \frac{n_1 n_2}{\sqrt{n_1^2 + n_2^2}}, \quad (27)$$

$$\langle BSO(G_{\text{BR}}) \rangle \approx \sqrt{n_1^2 + n_2^2}, \quad (28)$$

$$\langle SO_\alpha(G_{\text{BR}}) \rangle \approx (n_1^\alpha + n_2^\alpha)^{1/\alpha} (n_1 n_2)^2 p^4, \quad (29)$$

$$\langle KA_{\alpha,\beta}^1(G_{\text{BR}}) \rangle \approx n_1 n_2 p [(n_1 p)^\alpha + (n_2 p)^\alpha]^\beta. \quad (30)$$

Above we used $|E(G_{\text{BR}})| = n_1 n_2 p$. In Figs. 5(a)-5(c), we show that Eqs. (26-28) (black-dashed lines) indeed describe well the data (thick full curves) for large enough p .

As for ER graphs, here for BR graphs the average modified Sombor index and the average first Banhatti-Sombor index do not depend on the probability p in the dense limit, see Eqs. (27,28). Also, by recognizing the average degrees $\langle k_{1,2} \rangle$ in Eqs. (26,29,30), they can be rewritten as

$$\langle SO(G_{\text{BR}}) \rangle \approx \sqrt{n_1^2 + n_2^2} (\langle k_1 \rangle \langle k_2 \rangle)^2, \quad (31)$$

$$\langle SO_\alpha(G_{\text{BR}}) \rangle \approx (n_1^\alpha + n_2^\alpha)^{1/\alpha} (\langle k_1 \rangle \langle k_2 \rangle)^2, \quad (32)$$

$$\langle KA_{\alpha,\beta}^1(G_{\text{BR}}) \rangle \approx |E(G_{\text{BR}})| (\langle k_1 \rangle^\alpha + \langle k_2 \rangle^\alpha)^\beta. \quad (33)$$

Therefore, by plotting $\langle \overline{SO}(G_{\text{BR}}) \rangle$ vs. $\langle k_1 \rangle \langle k_2 \rangle$, $\langle {}^m \overline{SO}(G_{\text{BR}}) \rangle$ vs. p , and $\langle \overline{BSO}(G_{\text{BR}}) \rangle$ vs. p [with $\langle \overline{SO}(G_{\text{BR}}) \rangle = \langle SO(G_{\text{BR}}) \rangle / \sqrt{n_1^2 + n_2^2}$, $\langle {}^m \overline{SO}(G_{\text{BR}}) \rangle = \sqrt{n_1^2 + n_2^2} \langle {}^m SO(G_{\text{BR}}) \rangle / (n_1 n_2)$, and $\langle \overline{BSO}(G_{\text{BR}}) \rangle = \langle BSO(G_{\text{BR}}) \rangle / \sqrt{n_1^2 + n_2^2}$], see Figs. 5(d-f), we confirm that the curves of these average Sombor indices on BR graphs coincide in the dense limit, as predicted by Eqs. (31), (27) and (28), respectively.

It is relevant to stress that, while the curves $\langle {}^m \overline{SO}(G_{\text{BR}}) \rangle$ vs. p and $\langle \overline{BSO}(G_{\text{BR}}) \rangle$ vs. p are properly normalized on the vertical axis, they are still not scaled on the p -axis. That is, the curves of the main panels in Figs. 5(e,f) do not coincide. However, through a standard scaling analysis (not shown here), it is possible to find the scaling parameter

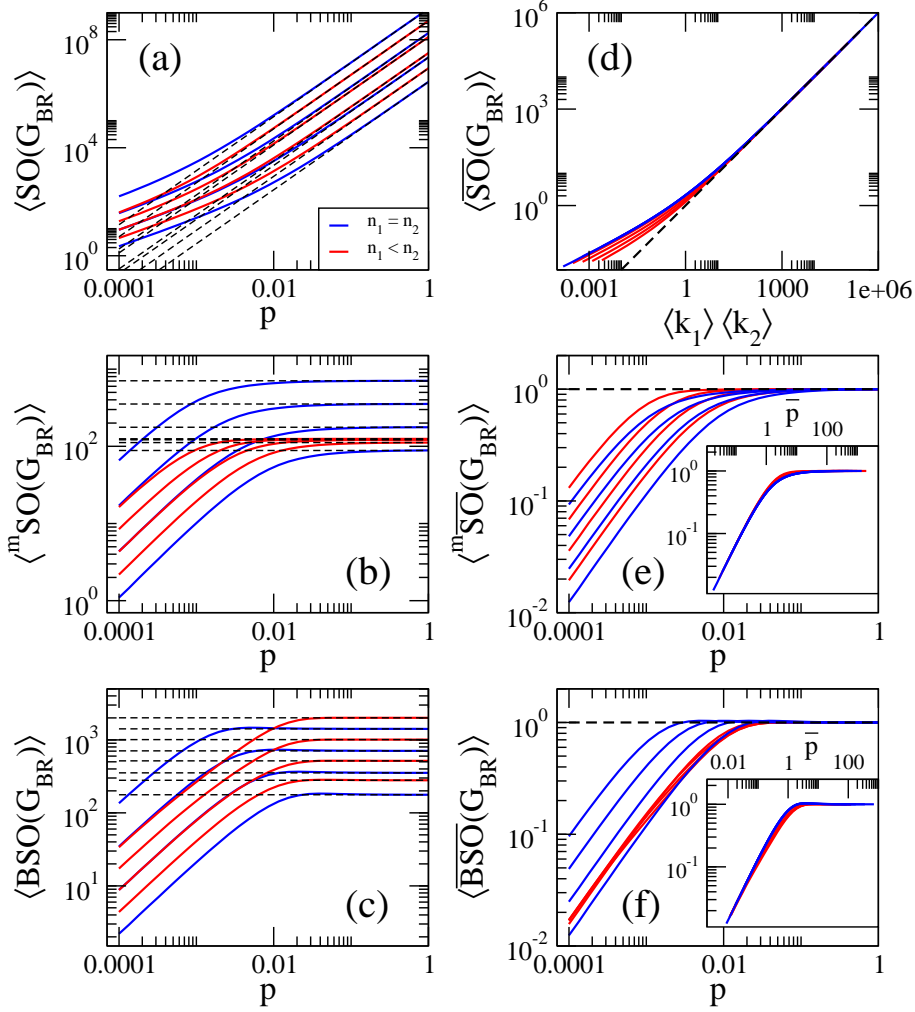


Figure 5. (a) Average Sombor index $\langle SO(G_{BR}) \rangle$, (b) average modified Sombor index $\langle {}^m SO(G_{BR}) \rangle$, and (c) average first Bhatti-Sombor index $\langle BSO(G_{BR}) \rangle$ as a function of the probability p of bipartite random graphs with sets of sizes n_1 and n_2 . In all panels: $n_1 = n_2$ with $n_2 = \{125, 250, 500, 1000\}$ (blue lines, n_2 increases from bottom to top) and $n_1 < n_2$ with $n_1 = 125$ and $n_2 = \{250, 500, 1000, 2000\}$ (red lines, n_2 increases from bottom to top). (d) $\langle \overline{SO}(G_{BR}) \rangle = \langle SO(G_{BR}) \rangle / \sqrt{n_1^2 + n_2^2}$ vs. the product $\langle k_1 \rangle \langle k_2 \rangle$. (e) $\langle {}^m \overline{SO}(G_{BR}) \rangle = \sqrt{n_1^2 + n_2^2} \langle {}^m SO(G_{BR}) \rangle / (n_1 n_2)$ vs. p . (f) $\langle \overline{BSO}(G_{BR}) \rangle = \langle BSO(G_{BR}) \rangle / \sqrt{n_1^2 + n_2^2}$ vs. p . Dashed lines in panels (a), (b) and (c) correspond to Eqs. (26), (27) and (28), respectively. While dashed lines in panels (d), (e) and (f) are Eqs. (31), (27) and (28), respectively. The inset in (e) shows $\langle {}^m \overline{SO}(G_{BR}) \rangle$ vs. $\bar{p} = p\sqrt{n_1^2 + n_2^2}$. The inset in (f) shows $\langle \overline{BSO}(G_{BR}) \rangle$ vs. $\bar{p} = pn_1 n_2 / \sqrt{n_1^2 + n_2^2}$.

p^* such that the curves $\langle {}^m \overline{SO}(G_{BR}) \rangle$ vs. \bar{p} and $\langle \overline{BSO}(G_{BR}) \rangle$ vs. \bar{p} , with $\bar{p} \equiv p/p^*$, fall on top of each other. Indeed, we found that $p^* = 1/\sqrt{n_1^2 + n_2^2}$ for $\langle {}^m \overline{SO}(G_{BR}) \rangle$ and $p^* = \sqrt{n_1^2 + n_2^2}/(n_1 n_2)$ for $\langle \overline{BSO}(G_{BR}) \rangle$. Thus, as can be seen in the insets of Figs. 5(e,f), the curves of the main panels are now properly scaled when plotted as a function of \bar{p} .

It is remarkable to notice that in the case of $n_1 = n_2 = n/2$, where $\langle k_1 \rangle = \langle k_2 \rangle =$

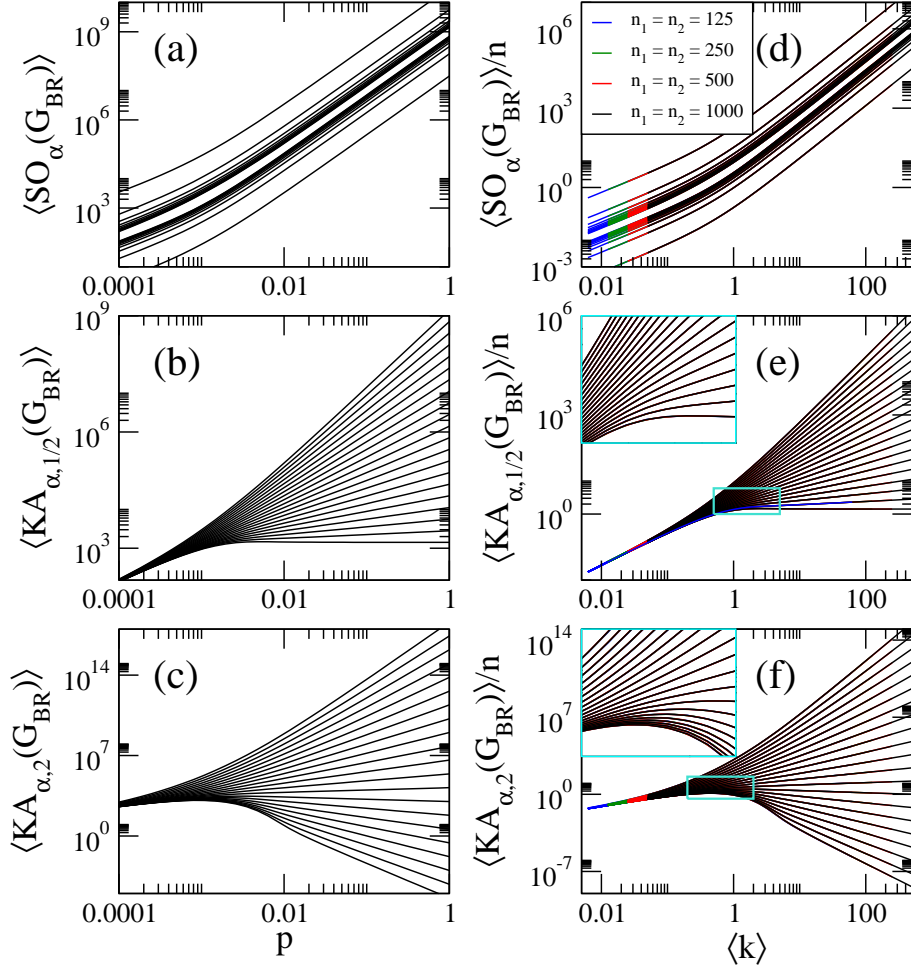


Figure 6. (a) Average α -Sombor index $\langle SO_\alpha(G_{BR}) \rangle$, (b) average first (α, β) - KA index $\langle KA_{\alpha,\beta}(G_{BR}) \rangle$, with $\beta = 1/2$, and (c) average first (α, β) - KA index $\langle KA_{\alpha,\beta}(G_{BR}) \rangle$, with $\beta = 2$, as a function of the probability p of bipartite random graphs with sets of sizes $n_1 = n_2 = 1000$. In all panels we show curves for $\alpha \in [-2, 2]$ in steps of 0.2 (from bottom to top). (d) $\langle SO_\alpha(G_{BR}) \rangle / n$, (e) $\langle KA_{\alpha,1/2}(G_{BR}) \rangle / n$, and (f) $\langle KA_{\alpha,2}(G_{BR}) \rangle / n$ as a function of $\langle k \rangle$ for BR graphs of four different sizes n . The insets in (e,f) are enlargements of the cyan rectangles.

$\langle k \rangle = np/2$, we get exactly the same expressions listed in Eqs. (13-17). This is verified in Figs. 6(d-f) where we plot average Sombor indices on RG graphs, normalized to n , as a function of $\langle k \rangle$ showing that all curves are properly scaled.

3 General scaling of Sombor indices on random graphs

In the previous Section we have shown that the average value of Sombor indices, normalized to the graph size, scale with the average degree $\langle k \rangle$ of the corresponding random graph models; we note that this also applies to BR graphs when $n_1 = n_2$. This

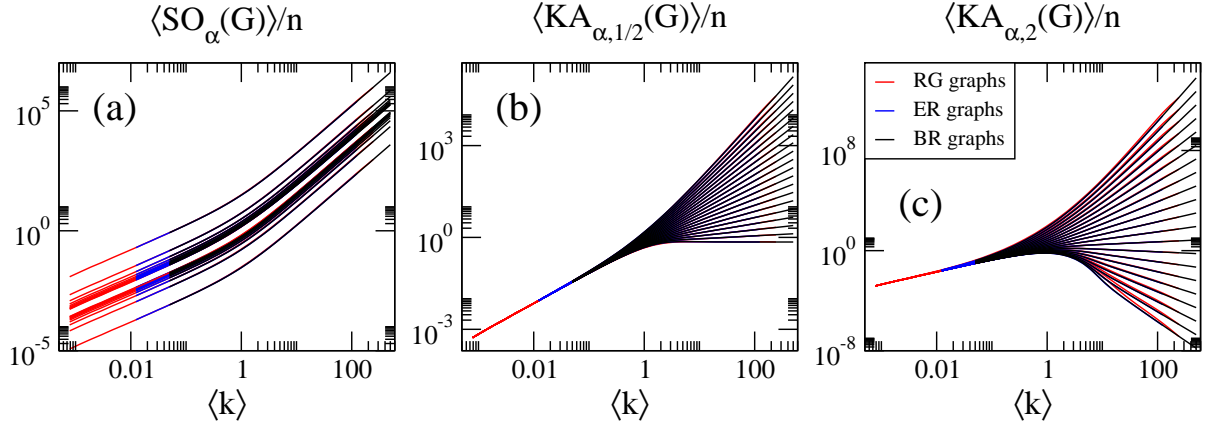


Figure 7. (a) $\langle SO_\alpha(G) \rangle / n$, (b) $\langle KA_{\alpha,1/2}(G) \rangle / n$, and (c) $\langle KA_{\alpha,2}(G) \rangle / n$ as a function of the average degree $\langle k \rangle$ for RG, ER, and BR graphs. In all panels we show curves for $\alpha \in [-2, 2]$ in steps of 0.2 (from bottom to top).

means that $\langle k \rangle$ fixes the average value of any Sombor index for different combinations of graph parameters; i.e. the relevant parameter of the random graph models we study here is $\langle k \rangle$ and not the specific values of the model parameters. This result highlights the relevance of $\langle k \rangle$ in random graph studies. Moreover, the applicability of Eqs. (13-17) to the three random graph models we study here allow us to relate the average value of a given Sombor index X of the three random graph models as

$$\frac{\langle X(G_{\text{ER}}) \rangle}{n} \approx \frac{\langle X(G_{\text{RG}}) \rangle}{n} \approx \frac{\langle X(G_{\text{BR}}) \rangle}{n} \quad \text{if} \quad \langle k_{\text{ER}} \rangle \approx \langle k_{\text{RG}} \rangle \approx \langle k_{\text{BR}} \rangle, \quad (34)$$

where $\langle k_{\text{ER}} \rangle$, $\langle k_{\text{RG}} \rangle$, and $\langle k_{\text{BR}} \rangle$ are given in Eqs. (6), (19), and (25), respectively.

Now, to verify Eq. (34), in Fig. 7 we compare normalized Sombor indices, $\langle X(G) \rangle / n$, for ER, RG, and BR graphs, as a function of the corresponding $\langle k \rangle$. Note that to really put Eq. (34) to test, we are using graphs of different sizes. Indeed, we observe that Eq. (34) is satisfied to a good numerical accuracy; that is, we observe the coincidence of the curves $\langle X(G) \rangle / n$ vs. $\langle k \rangle$ corresponding to different graphs models.

4 Sombor indices as complexity measures for random graphs

Additionally, we want to recall that in complex systems research there is a continuous search of measures that could serve as complexity indicators. In particular, random matrix theory (RMT) has provided us with a number of measures able to distinguish between (i) integrable and chaotic (i.e. non-integrable) and (ii) ordered and disordered

quantum systems [35, 36]. Such measures are computed from the eigenvalues and eigenvectors of quantum Hamiltonian matrices. Examples of eigenvalue-based measures are the distribution of consecutive eigenvalue spacings, the spectrum rigidity and the ratios between consecutive eigenvalue spacings; while the inverse participation ratios and Shannon entropies are popular eigenvector-based complexity measures [35, 36]. It is interesting to notice that all these RMT measures have also been successfully applied to study networks and graphs since they can be computed from the eigenvalues and eigenvectors of adjacency matrices; see e.g. [37–39] and the references therein. Therefore, these measures are able to distinguish between graphs composed by mostly isolated vertices and mostly connected graphs. Also, through scaling studies of RMT measures it has been possible to locate the percolation transition point of random graphs models [37, 38]. It is worth mentioning that the scaling study of average Sombor indices performed in this paper has followed a *statistical* RMT approach; that is, from a detailed computational study we have been able to identify the average degree as the universal parameter of our random graph models: i.e. the parameter that fixes the average values of the Sombor indices.

Moreover, recently, it has been shown for RG graphs that there is a huge correlation between the average-scaled Shannon entropy (of the adjacency matrix eigenvectors) and two average-scaled topological indices [40]: the Randić index $R(G)$ and the harmonic index $H(G)$. We believe that this is a remarkable result because it validates the use of average topological indices as RMT complexity measures; already suggested in Refs. [32, 33] for ER random networks. Now, it is important to stress that not every index could be used as a complexity measure. From our experience, we conclude that good candidates should fulfill a particular requirement: they should get well defined values in the trivial regimes (just as RMT measures are). For example, a useful complexity measure for random graphs should be close to zero in the regime of mostly isolated vertices while it should become constant above the percolation transition. Indeed, this is a property that both $\langle R(G) \rangle$ and $\langle H(G) \rangle$ have: $\langle R(G) \rangle \approx \langle H(G) \rangle \approx 0$ for mostly isolated vertices while $\langle R(G) \rangle / n \approx \langle H(G) \rangle / n \approx 1/2$ once the network is well above the percolation transition.

Therefore, a straightforward application of our study on Sombor indices is the identification of specific Sombor indices as complexity measure candidates. Recall that we particularly require, for an average-scaled Sombor index to work as complexity measure,

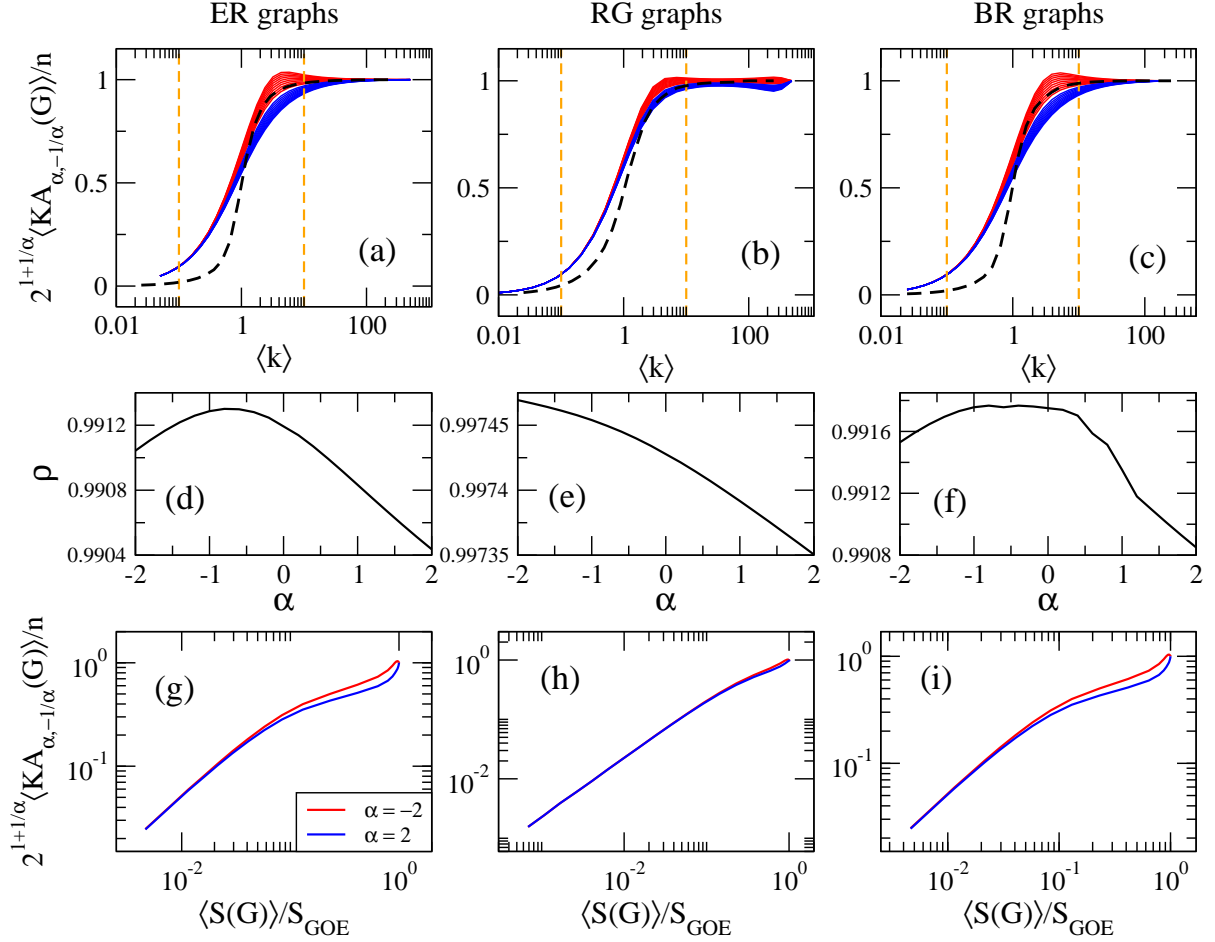


Figure 8. $2^{1+1/\alpha} \langle KA_{\alpha,-1/\alpha}^1(G) \rangle / n$ as a function of the average degree $\langle k \rangle$ for (a) ER graphs of size $n = 500$, (b) RG graphs of size $n = 500$, and (c) BR graphs with $n_1 = n_2 = 250$. In all panels we show curves for $\alpha \in [-2, 2]$ in steps of 0.2; except for $\alpha = 0$. Red (blue) lines correspond to $\alpha < 0$ ($\alpha > 0$). Vertical orange dashed-lines mark $\langle k \rangle = 1/10$ and $\langle k \rangle = 10$, see the text. Black-dashed lines in (a-c) correspond to the normalized Shannon entropies $\langle S(G) \rangle / S_{\text{GOE}}$. (d-f) Pearson's correlation coefficient ρ between $2^{1+1/\alpha} \langle KA_{\alpha,-1/\alpha}^1(G) \rangle / n$ and $\langle S(G) \rangle / S_{\text{GOE}}$ as a function of α . (g-i) Scatter plots of $2^{1+1/\alpha} \langle KA_{\alpha,-1/\alpha}^1(G) \rangle / n$ vs. $\langle S(G) \rangle / S_{\text{GOE}}$ for $\alpha = -2$ and 2.

that $\langle X(G) \rangle / n \approx \text{const.}$ for large enough $\langle k \rangle$. In fact, from Eqs. (14) and (15) we can see that the above condition is fulfilled for $\langle {}^m SO(G) \rangle$ and $\langle BSO(G) \rangle$, respectively. More generally, by properly choosing the values of α and β in Eq. (17) we could also use $\langle KA_{\alpha,\beta}(G) \rangle$ as complexity measure. Specifically, for $\beta = -1/\alpha$ we get

$$\frac{\langle KA_{\alpha,-1/\alpha}^1(G) \rangle}{n} \approx \frac{1}{2^{1+1/\alpha}}. \quad (35)$$

Note that $\langle KA_{\alpha,-1/\alpha}^1(G) \rangle$ reproduces both $\langle {}^m SO(G) \rangle$ and $\langle BSO(G) \rangle$ when $\alpha = 2$ and $\alpha = -2$, respectively. Thus, in Fig. 8 we plot $2^{1+1/\alpha} \langle KA_{\alpha,-1/\alpha}^1(G) \rangle / n$ as a

function of the average degree $\langle k \rangle$ for ER, RG, and BR graphs. From the behavior of the average-scaled indices reported in Fig. 8 we can identify three regimes: (i) a regime of mostly isolated vertices when $\langle k \rangle < 1/10$, where $2^{1+1/\alpha} \langle KA_{\alpha,-1/\alpha}^1(G) \rangle / n \approx 0$, (ii) a regime corresponding to mostly connected graphs when $\langle k \rangle > 10$, where $2^{1+1/\alpha} \langle KA_{\alpha,-1/\alpha}^1(G) \rangle / n \approx 1$, and (iii) a transition regime in the interval $1/10 < \langle k \rangle < 10$, which is logarithmically symmetric around the percolation transition point $\langle k \rangle \approx 1$. Accordingly, we propose the use of $\langle KA_{\alpha,-1/\alpha}^1(G) \rangle$ as complexity measure for random graph models.

4.1 Correlation between the average $KA_{\alpha,-1/\alpha}^1(G)$ index and the average Shannon entropy

Since we are proposing the use of $\langle KA_{\alpha,-1/\alpha}^1(G) \rangle$ as a complexity measure for random graphs, it is pertinent to compare it to other standard RMT complexity measure. To this end we choose the average Shannon entropy $\langle S \rangle$ of the adjacency matrix eigenvectors.

In particular we construct randomly weighted adjacency matrices, see e.g. [40], such that we obtain well-known RMT ensembles in the limits of: (i) isolated vertices (where we get random diagonal adjacency matrices, known in RMT as the Poisson ensemble) and (ii) complete graphs (where the adjacency matrices become members of the Gaussian Orthogonal Ensemble (GOE)). Specifically, for the normalized eigenvector Ψ^i , i.e. $\sum_{j=1}^n |\Psi_j^i|^2 = 1$, S is defined as

$$S_i = - \sum_{j=1}^n |\Psi_j^i|^2 \ln |\Psi_j^i|^2 . \quad (36)$$

Then, we use exact numerical diagonalization to obtain the eigenvectors Ψ^i ($i = 1, \dots, n$) of large ensembles of adjacency matrices and compute $\langle S \rangle$, where the average is taken over all the eigenvectors of all the adjacency matrices of the ensemble.

In Figs. 8(a-c) we present $\langle S(G) \rangle$, normalized to $S_{\text{GOE}} \approx \ln(n/2.07)$, for ER, RG and BR graphs; see the black-dashed lines. From these figures one can observe that $\langle KA_{\alpha,-1/\alpha}^1(G) \rangle$ and $\langle S(G) \rangle$ are indeed highly correlated. To quantify the correlation, in panels Figs. 8(d-f) we report the corresponding Pearson's correlation coefficient ρ , which turns out to be approximately equal to one for all the values of α we consider. Finally, to validate the high correlation reported by ρ , in Figs. 8(g-i) we show two examples of scatter plots of $2^{1+1/\alpha} \langle KA_{\alpha,-1/\alpha}^1(G) \rangle / n$ vs. $\langle S(G) \rangle / S_{\text{GOE}}$.

5 Conclusions

In this paper we have performed a thorough computational study of Sombor indices on random graphs. As models of random graphs we have used Erdős-Rényi graphs, random geometric graphs, and bipartite random graphs.

Within a statistical random matrix theory approach, we show that the average values of Sombor indices, normalized to the order of the graph n , scale with the graph average degree $\langle k \rangle$. Thus, we conclude that $\langle k \rangle$ is the parameter that fixes the average values of Sombor indices on random graphs. Moreover, it is remarkable that we were able to state a scaling law that includes different graph models; see Eq. (34) and Fig. 7.

Moreover, we discuss the application of Sombor indices as complexity measures of random graphs and, as a consequence, we show that the average first $(\alpha, \beta) - KA$ index (with $\beta = -1/\alpha$), normalized to n , is highly correlated with the averaged-scaled Shannon entropy of the eigenvectors of the graph adjacency matrix. That is, $\langle KA_{\alpha, -1/\alpha}^1(G) \rangle / n$ may serve as complexity measure for random graph models.

We hope that our work may motivate further analytical as well as computational studies of Sombor indices on random graphs.

ACKNOWLEDGEMENTS

The research of J.M.R. and J.M.S. was supported by a grant from Agencia Estatal de Investigación (PID2019-106433GB-I00/AEI/10.13039/501100011033), Spain. J.M.R. was supported by the Madrid Government (Comunidad de Madrid-Spain) under the Multiannual Agreement with UC3M in the line of Excellence of University Professors (EPUC3M23), and in the context of the V PRICIT (Regional Programme of Research and Technological Innovation).

References

- [1] I. Gutman, Geometric approach to degree-based topological indices: Sombor indices. *MATCH Commun. Math. Comput. Chem.* **86**, 11–16 (2021).
- [2] V. R. Kulli and I. Gutman, Computation of Sombor indices of certain networks, *SSRG Int. J. Appl. Chem.* **8**, 1–5 (2021).

- [3] Z. Lina, T. Zhou, V. R. Kullić, and L. Miao, On the first Banhatti-Sombor index, preprint arXiv:2104.03615.
- [4] T. Reti, T. Doslic, and A. Ali, On the Sombor index of graphs, *Contrib. Math.* **3**, 11–18 (2021).
- [5] V. R. Kulli, The (a, b) - KA indices of polycyclic aromatic hydrocarbons and benzenoid systems, *International Journal of Mathematics Trends and Technology* **65**, 115–120 (2019).
- [6] B. Zhou and N. Trinajstić, On general sum-connectivity index, *J. Math. Chem.* **47**, 210–218 (2010).
- [7] V. R. Kulli, δ -Sombor index and its exponential for certain nanotubes, *Annals of Pure and Applied Mathematics*, in press (2021).
- [8] R. Cruz, I. Gutman, and J. Rada, Sombor index of chemical graphs, *Appl. Math. Comput.* **399**, 126018 (2021).
- [9] R. Cruz and J. Rada, Extremal values of the Sombor index in unicyclic and bicyclic graphs, *J. Math. Chem.* **59**, 1098–1116 (2021).
- [10] N. Ghanbari and S. Alikhani, Sombor index of certain graphs, preprint arXiv:2102.10409.
- [11] S. Alikhani and N. Ghanbari, Sombor index of polymers, *MATCH Commun. Math. Comput. Chem.* **86**, 715–728 (2021).
- [12] X. Fang, L. You, and H. Liu, The expected values of Sombor indices in random hexagonal chains, phenylene chains and Sombor indices of some chemical graphs, preprint arXiv:2103.07172.
- [13] H. Deng, Z. Tang, and R. Wu, Molecular trees with extremal values of Sombor indices, *Quantum Chemistry*, in press (2021).
- [14] H. Liu, Ordering chemical graphs by their Sombor indices, preprint arXiv:2103.05995.
- [15] H. Liu, Maximum Sombor index among cacti, preprint arXiv:2103.07924.

- [16] H. Liu, L. You, Y. Huang, Ordering chemical graphs by Sombor indices and its applications, *MATCH Commun. Math. Comput. Chem.* **86** (2021) in press.
- [17] T. Zhou, Z. Lin, and L. Miao, The Sombor index of trees and unicyclic graphs with given matching number, preprint arXiv:2103.04645.
- [18] T. Zhou, Z. Lin, and L. Miao, The Sombor index of trees and unicyclic graphs with given maximum degree, preprint arXiv:2103.07947.
- [19] I. Gutman, Some basic properties of Sombor indices, *Open J. Discret. Appl. Math.* **4**, 1–3 (2021).
- [20] I. Milovanovic, E. Milovanovic, and M. Mateji, On some mathematical properties of Sombor indices, *Bull. Int. Math. Virtual Inst.* **11**, 341–353 (2021).
- [21] K. C. Das, A. S. Cevik, I. N. Cangul, and Y. Shang, On Sombor index, *Symmetry* **13**, 140 (2021).
- [22] J. Rada, J. M. Rodriguez, and J. M. Sigarreta, General properties on Sombor indices, *Discrete Applied Mathematics* **299**, 87–97 (2021).
- [23] I. Milovanović, E. Milovanović, A. Ali, and M. Matejić, Some results on the Sombor indices of graphs, *Contrib. Math.* **3**, 5–67 (2021).
- [24] Z. Wang, Y. Mao, Y. Li, and B. Furtula, On relations between Sombor and other degree-based indices, *J. Appl. Math. Comput.* (2021) in press.
- [25] I. Redzepovic, Chemical applicability of Sombor indices, *J. Serb. Chem Soc.* (2021) in press.
- [26] Z. Lin, On the spectral radius, energy and Estrada index of the Sombor matrix of graphs, preprint arXiv:2102.03960.
- [27] R. Solomonoff and A. Rapoport, Connectivity of random nets. *Bull. Math. Biophys.* **13**, 107–117 (1951).
- [28] P. Erdős and A. Rényi, On random graphs. *Publ. Math. (Debrecen)* **6**, 290–297 (1959).

- [29] P. Erdős and A. Rényi, On the evolution of random graphs, *Inst. of the Hung. Acad. of Sci.* **5**, 17–61 (1960); On the strength of connectedness of a random graph, *Acta Mathematica Hungarica* **12**, 261–267 (1961).
- [30] J. Dall and M. Christensen, Random geometric graphs, *Phys. Rev. E* **66**, 016121 (2002).
- [31] M. Penrose, *Random Geometric Graphs*; (Oxford University Press, Oxford, 2003).
- [32] C. T. Martínez-Martínez, J. A. Mendez-Bermudez, J. M. Rodríguez, and J. M. Sigarreta, Computational and analytical studies of the Randić index in Erdős–Rényi models, *Appl. Math. Comput.* **377**, 125137 (2020).
- [33] C. T. Martínez-Martínez, J. A. Mendez-Bermudez, J. M. Rodríguez, and J. M. Sigarreta, Computational and analytical studies of the harmonic index in Erdős–Rényi models, *MATCH Commun. Math. Comput. Chem.* **85**, 395–426 (2021).
- [34] E. Estrada and M. Sheerin, Random rectangular graphs, *Phys Rev. E* **91**, 042805 (2015).
- [35] M. L. Mehta, *Random Matrices* (Elsevier, Amsterdam, 2004).
- [36] F. Haake, *Quantum Signatures of Chaos* (Springer, Berlin, 2010).
- [37] J. A. Mendez-Bermudez, A. Alcazar-Lopez, A. J. Martinez-Mendoza, F. A. Rodrigues, and T. K. DM. Peron, Universality in the spectral and eigenfunction properties of random networks, *Phys. Rev. E* **91**, 032122 (2015).
- [38] L. Alonso, J. A. Mendez-Bermudez, A. Gonzalez-Melendrez, and Y. Moreno, Weighted random-geometric and random-rectangular graphs: Spectral and eigenfunction properties of the adjacency matrix, *J. Complex Networks* **6**, 753 (2018).
- [39] G. Torres-Vargas, R. Fossion, and J. A. Mendez-Bermudez, Normal mode analysis of spectra of random networks, *Physica A* **545**, 123298 (2020).
- [40] R. Aguilar-Sanchez, J. A. Mendez-Bermudez, F. A. Rodrigues, and J. M. Sigarreta-Almira, Topological versus spectral properties of random geometric graphs, *Phys. Rev. E* **102**, 042306 (2020).